SAND2023-11192J

Earth and Space Science

RESEARCH ARTICLE
10.1029/2023EA003149

Key Points:

- First direct observation of an elevated acoustic duct using an airborne acoustic source and receiver
- Detections provide insight into the characteristics of signals from ascending and descending supersonic objects
- Lack of detections on ground-based stations highlights the advantages of using balloon-borne sensors to detect sources at altitude

Correspondence to:
S. A. Albert,
salber@sandia.gov

Citation:
Albert, S. A., Bowman, D. C., Silber, E. A., & Dannemann Dugick, F. K. (2023). The AtmoSOFAR channel: First direct observations of an elevated acoustic duct. *Earth and Space Science*, *10*, e2023EA003149. https://doi.org/10.1029/2023EA003149

Received 5 JUL 2023
Accepted 14 SEP 2023

Author Contributions:

Conceptualization: S. A. Albert, D. C. Bowman
Data curation: D. C. Bowman
Formal analysis: S. A. Albert, E. A. Silber, F. K. Dannemann Dugick
Funding acquisition: S. A. Albert
Methodology: S. A. Albert, D. C. Bowman
Validation: S. A. Albert, D. C. Bowman, E. A. Silber, F. K. Dannemann Dugick
Visualization: S. A. Albert
Writing – original draft: S. A. Albert
Writing – review & editing: S. A. Albert, D. C. Bowman, E. A. Silber, F. K. Dannemann Dugick

The AtmoSOFAR Channel: First Direct Observations of an Elevated Acoustic Duct

S. A. Albert[1], D. C. Bowman[1], E. A. Silber[1], and F. K. Dannemann Dugick[1]

[1]Sandia National Laboratories, Albuquerque, NM, USA

Abstract The Sound Fixing and Ranging (SOFAR) channel in the ocean allows for low frequency sound to travel thousands of kilometers, making it particularly useful for detecting underwater nuclear explosions. Suggestions that an elevated SOFAR-like channel should exist in the stratosphere date back over half a century and imply that sources within this region can be reliably sensed at vast distances. However, this theory has not been supported with evidence of direct observations from sound within this channel. Here we show that an infrasound sensor on a solar hot air balloon recorded the first infrasound detection of a ground truth airborne source while within this acoustic channel, which we refer to as the AtmoSOFAR channel. Our results support the existence of the AtmoSOFAR channel, demonstrate that acoustic signals can be recorded within it, and provide insight into the characteristics of recorded signals. Results also show a lack of detections on ground-based stations, highlighting the advantages of using balloon-borne infrasound sensors to detect impulsive sources at altitude.

Plain Language Summary A layer exists in the ocean that allows sound to travel great distances. Something like this could exist in our atmosphere, too, but until now no one had verified this. Low frequency sound, known as infrasound, travels efficiently through the atmosphere. Specialized instruments, called infrasound sensors, are microphones that can record low frequency sound. We attached an infrasound sensor to a solar hot air balloon to make the first recording of a known object within the theorized atmospheric layer. Our results show that this layer exists, sound can be recorded within it, and analysis can give us more information about what generated that sound. The rocket launch was not well recorded by infrasound sensors on the ground, highlighting the advantages of our method for detecting objects that travel through this region of the atmosphere.

1. Introduction

The Sound Fixing and Ranging (SOFAR) channel in the ocean allows for sound to travel thousands of kilometers, making it particularly useful for detecting underwater nuclear explosions (Lawrence, 1999). The SOFAR-like, omnidirectional, acoustic duct in the atmosphere was first modeled over 15 years ago (Drob et al., 2003). Similar to the ocean, this acoustic duct corresponds to an area of minimum effective sound speed. Propagation modeling suggests that infrasound (with frequencies <20 Hz) generated at altitude and traveling within the acoustic channel would be less attenuated and more readily detected at further ranges (Bowman et al., 2018; Young et al., 2018). Therefore, high-altitude sources such as meteoroid airbursts and supersonic vehicles passing through this region should be reliably sensed at vast distances (possibly over 1,000 km) using an airborne receiver. Figure 1 shows an infographic of this duct, herein referred to as the AtmoSOFAR channel. Note the presence of an acoustic duct that spans altitudes of 10–40 km. In this example, a hypothetical source at ~30 km altitude generates an infrasound signal that gets trapped within the acoustic duct. Infrasound from that source propagates to a balloon-borne receiver, also situated within the channel, at ~25 km altitude.

The use of balloons for infrasound monitoring was first attempted over 50 years ago (Weaver & McAndrew, 1995; Wescott, 1964). However, until recently their potential was largely unexplored. From 2014 to 2016 researchers participating in the High Altitude Student Platform opportunity through the National Aeronautics and Space Administration (NASA) Balloon Program Office and Louisiana Space Consortium proved that acoustic data collection was possible at stratospheric altitudes (Bowman, 2016; Bowman & Lees, 2016). Two more zero pressure balloon experiments followed: the Stratospheric Infrasound Sensitivity Experiment (SISE) and the UNC-Sandia Infrasound Experiment (USIE) (Young et al., 2018). The SISE and USIE geoacoustics payloads detected infrasound signals from three 2,400 lb trinitrotoluene (TNT) equivalent (1 TNT = $4.184 \cdot 10^9$ J)

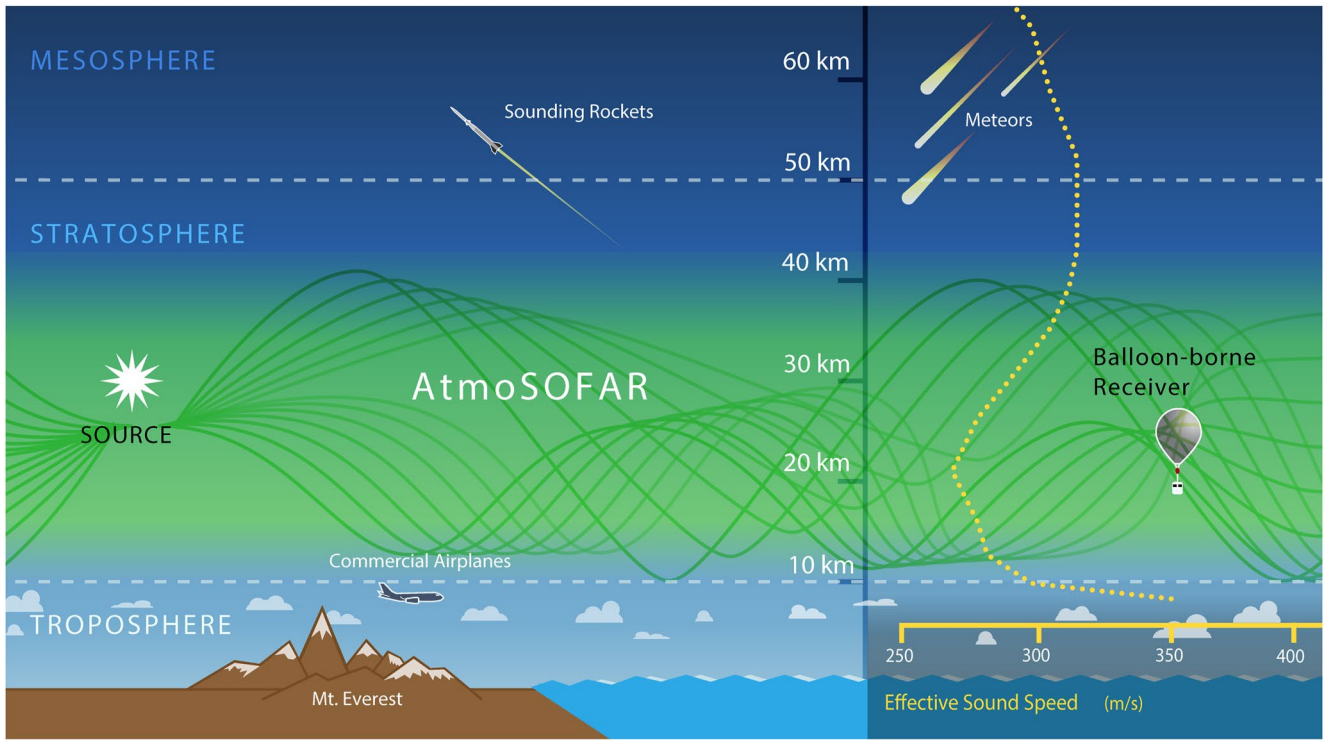

Figure 1. The AtmoSOFAR channel: an omnidirectional acoustic duct that spans altitudes of 10–40 km. In this example, there is a source at 30 km altitude. Infrasound from the source (green oscillating lines) gets trapped within the AtmoSOFAR channel and is recorded by a balloon-borne receiver at a similar altitude.

explosions on balloon-borne infrasound sensors up to 395 km from the source. Also during the USIE experiment, an infrasound sensor was launched on a prototype solar hot air balloon that would ultimately lead to the heliotrope design used in the present study. This sensor detected one of the explosions at approximately 300 km range. On the ground, explosions were recorded out to a distance of ∼176 km. This showed that balloon-borne measurements can provide detections at greater distances than equivalent single sensors on the ground. An infrasound sensor was also placed on a NASA Ultra Long Duration Balloon flight in 2016 and constantly recorded the microbarom, a signal that naturally occurs due to ocean processes, over a 17-day period (Bowman & Lees, 2018). A constant recording of the microbarom is unusual at the ground surface because of wind noise, suggesting that sensors at altitude are more sensitive than those at the ground surface due to the environment in which they operate in. These experiments led to the Heliotrope experiment where Bowman and Albert (2018) launched a network of five heliotrope solar balloons to create a sparse array in the sky. This array maintained an approximately 50–100 km horizontal aperture for several hours and at altitudes from ∼21 to 24 km above sea level. The array detected an 800 lb TNT equivalent explosion. The calculated backazimuth from this detection matched the true source-to-receiver backazimuth, showing promise for infrasound source location using a balloon-borne mirobarometer network.

At present, operational infrasound networks are solely ground based (Alaska Volcano Observatory, 2016; Bondár et al., 2022; Burlacu et al., 2010; Christie & Campus, 2010; Marty, 2019). They can record sound waves from distant sources only when the stratospheric winds are favorable, or when the signal is sufficiently low frequency to permit transmission from the thermosphere. Wind noise is a major issue for surface sensors and often reduces their effectiveness. Raspet et al. (2019) state that "*the greatest impediment to the detection and analysis of infrasound signals are the intrinsic pressure fluctuations due to air turbulence*, *known as wind noise*, *always present in the atmosphere*." Infrasound sensors at altitude have been shown to be lower noise than ground-based sensors because the balloon drifts with the wind, eliminating the wind noise described above. In fact, the USIE experiment showed an almost two orders of magnitude reduction in noise power on the solar hot air balloon and an almost three orders of magnitude reduction in noise power on the zero pressure balloon (likely due to its higher altitude).

Theory suggests that the AtmoSOFAR channel almost always exists, as it forms as a result of the local sound speed maximum produced by prevailing winds and average temperatures in the stratosphere (Young et al., 2016). Acoustic ray tracing models show that this duct efficiently captures acoustic waves from events in the upper troposphere or lower stratosphere. Therefore, meteoroid airbursts at these altitudes and supersonic vehicles passing through this region should be reliably sensed at global distances using balloon-borne infrasound sensors floating near the tropopause, which is ∼10–15 km altitude at the latitude in this study (Holton et al., 1995). In this manuscript we (a) present the first infrasound detection of a ground truth high-altitude airborne source on an airborne receiver within the AtmoSOFAR channel, (b) provide insight into the characteristics of recorded signals, and (c) highlight the advantages of using balloon-borne infrasound sensors over ground-based stations to detect sources at altitude.

2. Methods

2.1. Heliotrope Solar Hot Air Balloon

The heliotrope is a solar-powered hot air balloon that can carry scientific payloads into the upper troposphere and lower stratosphere (14–24 km altitude, depending on the design). The advantage of this design is that it can fly for multiple hours, terminating only during sunset. Payloads ranging from hundreds of grams to several kilograms can fly on a heliotrope. The design is relatively simple and low cost, making it ideal for a variety of applications. More detailed information on the heliotrope design, construction, trajectory, and flight characteristics is available in Bowman et al. (2020).

To capture acoustic signals, we launched a single 6 m "grand slam" heliotrope at dawn (∼07:00 local) out of Belen Regional Airport, NM, USA. The "grand slam" design utilizes a weather balloon to tow the heliotrope and scientific payload through non-ideal winds and/or low cloud cover. Two payloads were used, each containing one Gem Infrasound Logger infrasound sensor (Anderson et al., 2018). The Gem Infrasound Logger is an Arduino-based combination infrasound sensor and digitizer that is small, lightweight, inexpensive, and easy to deploy, making it particularly useful for balloon payloads. It has a flat response between 0.1 and 10 Hz (Slad & Merchant, 2021) and provides GPS time and location. Each sensor sampled data at 100 Hz. The two sensor payloads were connected via a reel-down system that was meant to separate the payloads by ∼90 m. However, the reel-down system did not deploy, essentially causing the payloads to be located only 2 m apart. Data from the bottom payload agrees with the top payload. We therefore focus on data from the top payload. Balloon trajectory was recorded using the GPS receiver on a High Altitude Science Eagle Flight Computer, which reports latitude, longitude, and altitude every 6 seconds. The Eagle Flight Computer was chosen for trajectory as it performs better at altitudes >18 km, where some GPS sensors fail. Data streams from the Gem Infrasound Loggers and Eagle Flight Computers were correlated using GPS time.

2.2. Blue Origin Rocket Launch

To record an acoustic source in the AtmoSOFAR channel, we made use of a publicly announced rocket launch. Blue Origin launched their NS-15 rocket out of West Texas, USA on 14 April 2021 around 16:51:00 UTC. The NS-15 launch was an uncrewed test flight of the space tourism rocket. This type of rocket reaches apogee at ∼100 km (above the Kármán Line) releases the capsule, and then the booster lands back on Earth's surface, essentially in the same place. On ascent, the rocket travels at supersonic velocities (Mach 1.4–1.5) with a curved edge leading the way and using jets for propulsion. On descent, the rocket travels at higher velocities (Mach 3.3 at 40 km altitude) but slows near the bottom of the channel (Mach 1.6 at 10 km altitude), when drag brakes are deployed. Therefore, for this specific launch, there are two instances where an object traversed the AtmoSOFAR channel, potentially injecting energy into it. Our balloon moved with an average velocity of 4.32 m/s. Therefore, at launch and during both the ascent and descent through the AtmoSOFAR channel, the rocket was at a range of 416 km from our payload. The closest ground-based stations were single sensors at ranges of 313–501 km (121A, ABTX, and MSTX), while the closest infrasound arrays were 1,047–1,303 km from the source (BRP, NOQ, BGU, EPU, and I57H). Locations of the rocket, heliotrope balloon with payload, and infrasound stations are shown in Figure 2a. The heliotrope's altitude with time is shown in Figure 2b. Note that the sharp ascent and peak above 25 km are a result of the grand slam design described in the previous section. It is also important to note that the rocket's liftoff time is only known to the minute, as Blue Origin did not release a more precise time.

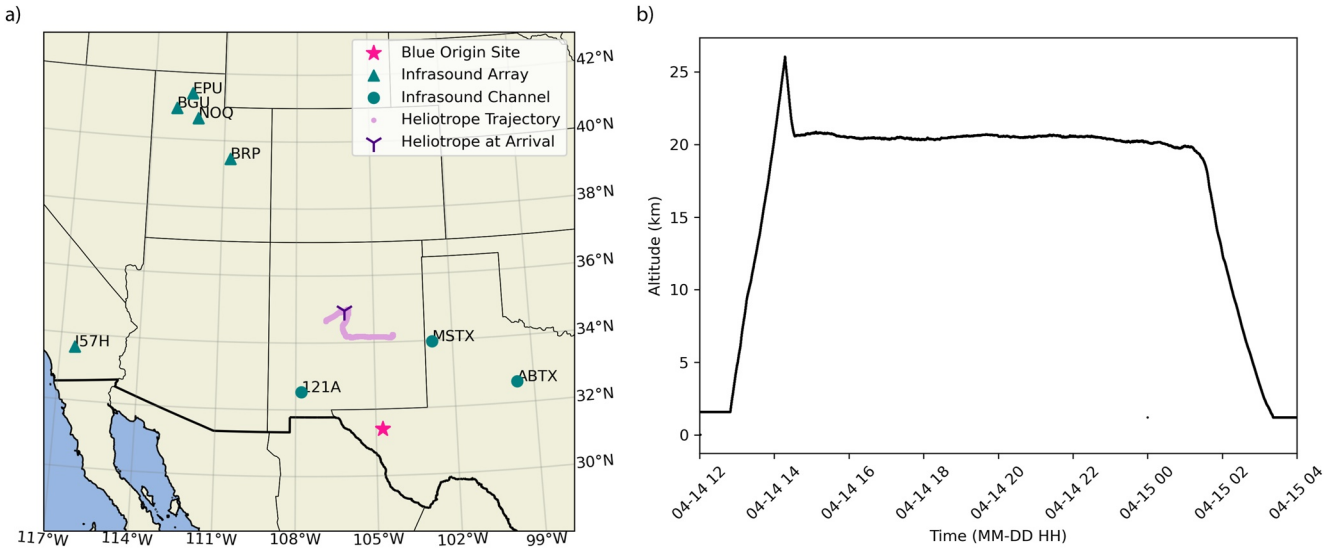

Figure 2. (a) Station map indicating the rocket, heliotrope, and ground-based infrasound station locations. The Blue Origin NS-15 rocket launch/ascent/descent location is denoted by a pink star, the full heliotrope trajectory by the plum line, the heliotrope location during the signal arrivals by a purple "Y," and the infrasound stations by teal circles (single-channel) or triangles (arrays). (b) Altitude with time for the heliotrope trajectory. The sharp ascent and peak above 25 km are a result of the grand slam design, which utilizes a weather balloon to tow the heliotrope in nonideal conditions.

Other information related to the launch, such as the timing of entrance into the AtmoSOFAR channel on both ascent and descent, was identified using the archived Blue Origin NS-15 launch webcast (Blue Origin, 2021).

2.3. Propagation Modeling

InfraGA is a software for modeling the path of infrasound through the atmosphere in the geometric limit (Blom, 2014; Blom & Waxler, 2012). Of the available methods, 2D Stratified Cartesian was chosen and the "prop" option used to generate ray paths at various inclination angles (−89.5°–89.5°, in 0.5° steps) from a fixed source location, the Blue Origin launch point, toward a fixed receiver location, the balloon-borne infrasound sensor (azimuth = 341°), and calculating 2 bounces. Six different source altitudes were used, situating the source every 10 km between 0 and 50 km, to predict the presence of the AtmoSOFAR channel and estimate its vertical span on this day. This method computes ray paths by estimating the effective sound speed based on a given atmospheric profile. Atmospheric specification came from NRL-G2S, a semiempirical model that provides temperature and wind conditions up to ∼150 km (Drob et al., 2003). NRL-G2S provides atmospheric profiles at 6 hr resolution so we chose the one closest in time to the Blue Origin launch, 18:00 UTC on 14 April 2021. Propagation modeling served two purposes: (a) it gave us a prediction that the AtmoSOFAR channel was present at the time of the launch and (b) it was used to identify a signal arrival time window for data analysis. Arrival time windows were found by averaging raytracing results that fell within ±5 km of the source-receiver range and within the AtmoSOFAR channel (10–40 km). These were then converted to arrival times, using the minimum and maximum to bracket the arrival time window.

2.4. Data Analysis

Analysis aimed to identify three signals: the rocket launch, and its ascent and its descent through the AtmoSOFAR channel. Bandpass filter limits were selected between 0.7 and 20 Hz in 1/3 octave bands to span a broad frequency range. For each frequency band, we performed narrowband processing using the Bloodhound infrasound analysis software (Arrowsmith et al., 2018). Bloodhound uses a Multivariate Adaptive Learning Detector (MALD) framework that is designed to detect very low signal-to-noise ratio (SNR) arrivals. This is a useful framework as it allows for data processing outputs to be combined to produce ensemble detection statistics. The detection threshold is also dynamic as it is based off the background noise distribution of the data. For the MALD framework, data is first processed in time windows using a suitable data transform. For single station data from the balloon and closest ground infrasound stations, a short-term average long-term average ratio (STA/LTA) was

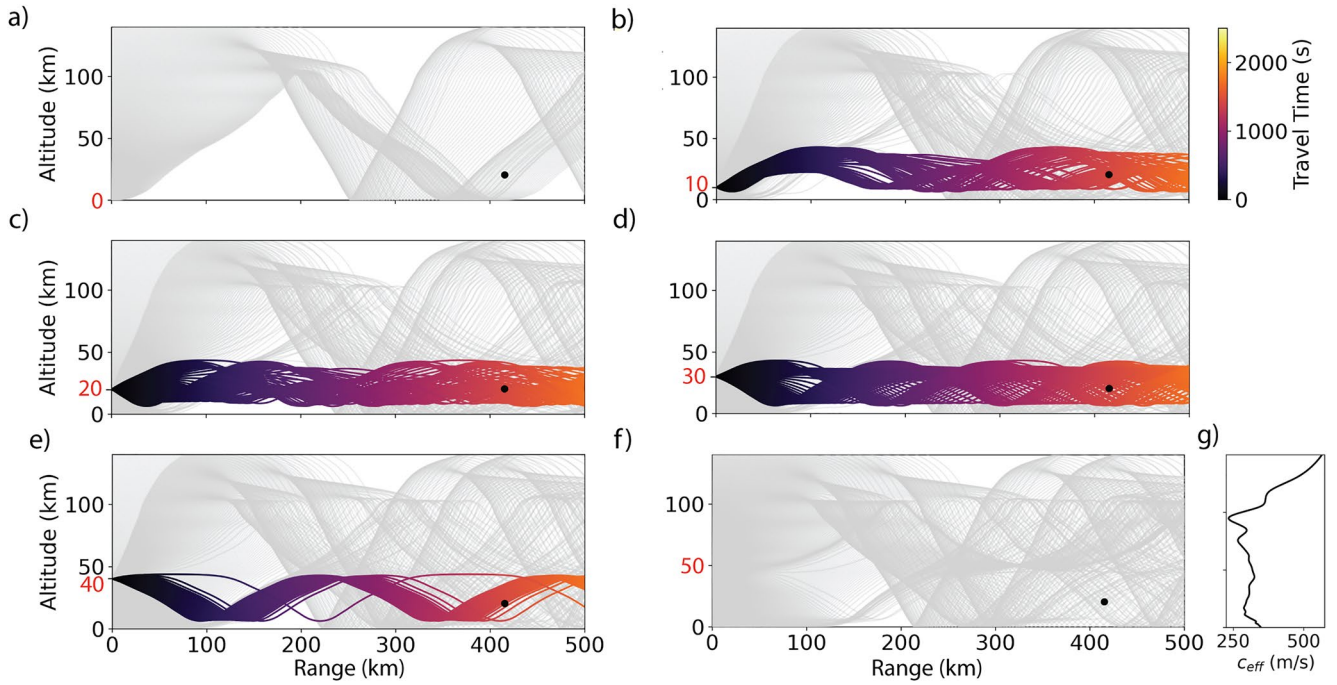

Figure 3. Modeled ray paths corresponding to a source at (a) 0, (b) 10, (c) 20, (d) 30, (e) 40, and (f) 50 km altitude (denoted by red font), and (g) the effective sound speed profile. Raypaths are colored by estimated travel time and balloon location is denoted by the black circle. Raypaths in panels (b–e) show the formation of the AtmoSOFAR channel spanning altitudes of 10–40 km. Raypaths with turning heights in the thermosphere and first bounce points on the ground are colored gray so as not to obscure the channel. Note that the balloon-borne infrasound sensor lies within the AtmoSOFAR channel in panels (b–e).

used. The STA and LTA windows were 3 and 60 s, respectively. A sliding window frequency-wavenumber (FK) processing was utilized for infrasound arrays (Rost & Thomas, 2002). Results from STA/LTA or FK processing were then converted to p-values using Kernel Density Estimation and Fisher's combined probability test. Detections were identified as those that fall below the *p*-value threshold provided by user input. For this study, the p-value detection threshold was set at 0.01. Processing was done for each frequency range and detections were aggregated across multiple frequency bands.

3. Results and Discussion

3.1. Balloon-Borne Receiver

First, it was necessary to use propagation modeling to predict the presence or absence of the AtmoSOFAR channel. By running propagation modeling for a source situated every 10 km between 0 and 50 km altitude and using the atmospheric profile noted above, we predicted that the AtmoSOFAR channel was present at the time of the Blue Origin launch and had a vertical span of ~10–40 km. This is shown in Figure 3a–3f by the ducting of sound when a source is situated within the 10–40 km altitude range. The effective sound speed profile is given in Figure 3g. Individual raypaths differ, but all sources at altitudes between 10 and 40 km inject energy into this channel, where it becomes trapped. Especially important is the fact that the balloon-borne infrasound sensor was within this region during the rocket launch (black dots in Figures 3b–3e), allowing us to verify the presence of the AtmoSOFAR channel. Below 10 km and above 40 km, sound is reflected away from the AtmoSOFAR channel. Thermospheric arrivals, with turning heights >100 km, are predicted to arrive on the ground for sources at all altitudes. Arrivals from the thermosphere are often not recorded due to high absorption rates (Sutherland & Bass, 2004). Therefore, in Figure 3 raypaths with turning heights in the thermosphere are colored gray so as not to obscure the channel. Raypaths with first bounce points on the ground are also colored gray for the same reason.

Propagation modeling was also used to identify travel times and corresponding signal arrival windows. A source height of 0 km corresponds to the Blue Origin rocket liftoff at roughly 16:51 UTC. Based on propagation modeling, signals are estimated to arrive 1,572–1,596 s later with turning heights in the thermosphere (Figure 3a).

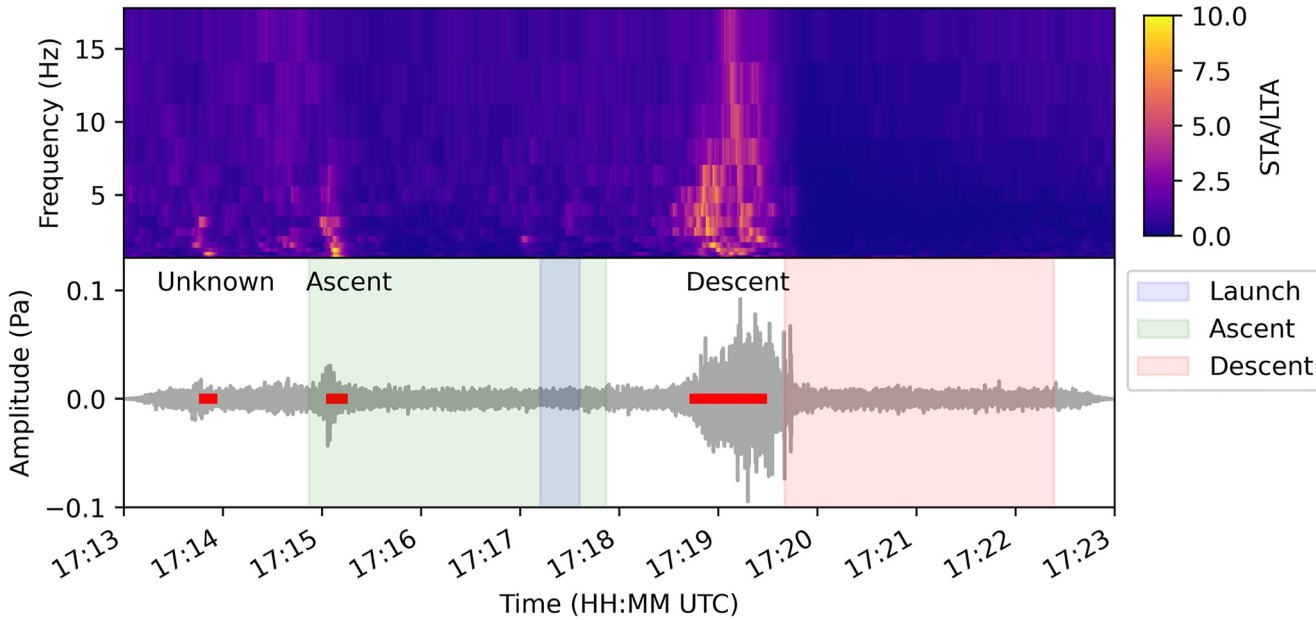

Figure 4. STA/LTA analysis and expected arrival time windows from the Blue Origin NS-15 rocket launch. Bloodhound detections are shown as red bars. The first detection arrives ~200 s earlier than expected from propagation modeling and is unlikely to be generated from the rocket. The other detections correspond to the rocket's ascent and descent through the AtmoSOFAR channel. Note that the characteristics of the descent signal are different than the other two.

Since the balloon-borne sensor was located after the first bounce point, a signal from the rocket liftoff is possible, but unlikely. On ascent, the rocket reached 10 km and entered the AtmoSOFAR channel around 16:52 UTC. Following apogee, the rocket entered the AtmoSOFAR channel from above at 40 km altitude around 16:57 UTC. Propagation modeling suggests signals arrived 1,360–1,483 s following the ascent and descent times mentioned above (Figures 3b–3e).

STA/LTA analysis using Bloodhound suggests the balloon-borne receiver recorded a signal at 17:13:48 UTC—1,368 s after launch. This signal arrives ~60 s earlier than expected from propagation modeling and corresponds to a celerity of 0.305 km/s. Therefore, we do not believe this is a signal from the Blue Origin NS-15 liftoff or path through the AtmoSOFAR channel and have labeled it "Unknown" in Figure 4. However, because we only had one receiver, it is difficult to verify this assertion. Multiple receivers would have allowed for signal cross-correlation and direction of arrival determination, which could help rule out a false detection.

More compelling, however, are the signals that followed the unknown signal. The signal from the rocket ascent through the AtmoSOFAR channel arrived 1,373 s following its entry into the channel, falling within the expected arrival time range calculated from propagation modeling (Figure 4, labeled "Ascent"). The rocket's descent signal arrived 1,305 s after entry into the AtmoSOFAR channel from above (Figure 4, labeled "Descent"). This is 55 s earlier than the expected window from propagation modeling, though this is likely due to the rocket booster's supersonic travel speed at this stage (further explained in the next paragraph). This signal has the highest SNR both 30 min before and after the window of interest (Figure 5). Because these signals correspond to expected arrival times and are high SNR, we are confident that these recordings correspond to signals that were ducted through the AtmoSOFAR channel and resulted from the booster's ascent and descent through it. Other unknown signals are present both before and after the time window we focused on for detecting the rocket arrivals, shown in Figure 5a. Much like the unknown signal in Figure 4, these unknown signals also have energy focused at frequencies less than 5 Hz and are lower SNR. Such signals are not unusual in balloon infrasound data and were also noted by Silber et al. (2023).

Comparing the three signals, the descent signal is different. It is higher SNR than the other two, spans a wider frequency range, and is longer duration. As described, the rocket travels at velocities of Mach 1.4–1.5 on ascent with a curved edge leading the way and using jets for propulsion. The jets are likely creating the signal in this instance. On descent, however, the rocket travels at Mach 3.3 at 40 km altitude and slows to Mach 1.6 at 10 km altitude, when drag brakes are deployed. The rocket does not fire again until just prior to landing, so the jets do

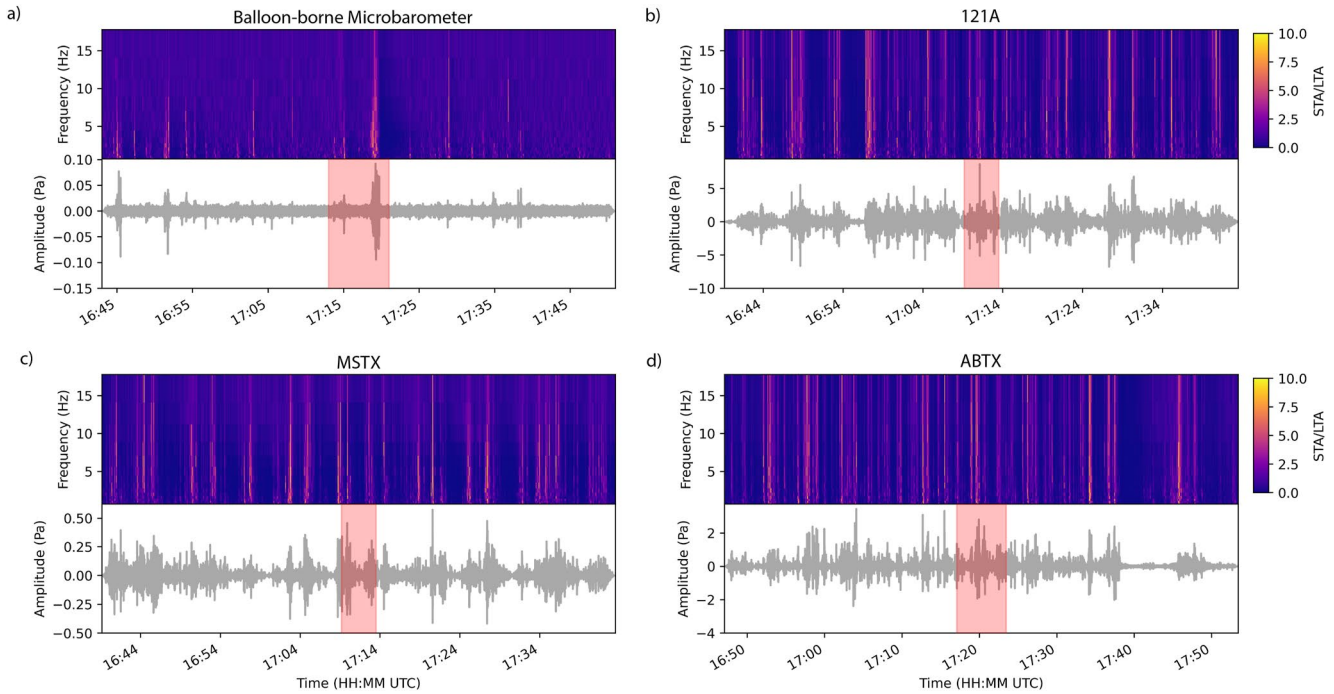

Figure 5. Background noise comparison between (a) the balloon-borne receiver and (b–d) the closest ground-based stations. The rocket launch signals are obvious on the balloon-borne sensor while noise dominates the signals on the ground. Station codes are listed in figure panel titles. Highlighted regions represent the expected signal arrival windows.

not generate a signal on descent. At this stage, the rocket is coming from above with a blunt edge leading the way, creating a broad shock carpet. Geometrically, the shock wave is not in an orientation conducive to horizontal propagation. Due to the blunt edge, the Mach cone is too wide, which directs the shock downward rather than outward. The early detection of the descent signal suggests that the downward propagating shock was trapped upon entering the AtmoSOFAR channel and subsequently recorded by our balloon-borne receiver. We do not record a shockwave, however, as the wave has already transitioned into the weak shock regime, resulting in Mach 1 velocities and linear propagation. Similar arrivals with energy concentrated at low frequencies and infrasonic velocities have been observed on ground-based stations from bolides (Pilger et al., 2018; Silber & Brown, 2019; Silber et al., 2011).

While these results show the first documented detection of an airborne source within the AtmoSOFAR channel on an airborne receiver, this data still suffers from limitations. First, we were limited by a single receiver. Ideally, future experiments should include multiple receivers at varying horizontal and vertical separations to improve detection and allow for source location. Vertical separation would also allow for the determination of signal direction of arrival (i.e., from above or below). This could be achieved by using multiple balloons with different payload weights (so they reach different altitudes of neutral buoyancy) or by separating two payloads on one balloon via a longer tether.

3.2. Ground-Based Receivers

Eight ground-based stations were also analyzed using the same method described in Section 2.4. We experimented with different p-value thresholds, but determined that varying inputs did not change the results. The closest ground stations were single sensors located at distances of 313–501 km: 121A (313 km), MSTX (340 km), and ABTX (501 km). These stations suffered from high background noise, which obscured any signals from the rocket. Unlike the balloon-borne receiver where the ascent and descent signals were obvious (Figure 5a), ground-based stations show numerous instances of high STA/LTA values within 30 min before and after the expected arrival time window (Figures 5b–5d).

Propagation modeling suggests that signals from the launch, ascent, and descent have thermospheric turning heights (>100 km). Because of this, these signals would be highly attenuated and very low SNR, likely falling below the background noise at these stations. Figure 6 shows turning heights and attenuation predicted by propagation modeling for all ground-based stations analyzed in this section. Results suggest there exist lower turning heights almost due East. These are likely due to the increase in effective sound speed (Figure 3g) and nature of the zonal winds just above 100 km altitude.

The closest infrasound arrays were located in Utah and California. The four arrays in Utah were 1,047–1,303 km from the rocket launch site: BRP (1,047 km), NOQ (1,222 km), BGU (1,291 km), and EPU (1,303 km). The array in California (I57H) was at a range of 1,126 km. Blue Origin arrivals may have been detected on the NOQ array, but there is no evidence of arrivals at the other stations. Again, propagation modeling suggests all arrivals should have thermospheric turning heights (>100 km) so they are unlikely to be detected (Figure 6). Sliding window FK analysis shows signals were detected within the expected window in some cases, but are from the wrong backazimuth for all but station NOQ. Figure 7 shows FK results for the arrays with the expected arrival time window highlighted by the red box. Station NOQ contains arrivals with energy concentrated at lower frequencies coming from the correct backazimuth. Trace velocities also correspond to ∼0.4 km/s—indicative of a signal refracted by the thermosphere.

The lack of detections on ground stations may be due to the nature of the source. Following launch, the greatest energy generated by the source at altitude is injected into the AtmoSOFAR channel, subsequently getting trapped there. This demonstrates the uniqueness of balloon-borne sensors for this type of signal detection—a single station in the AtmoSOFAR channel performs better than a single station on the ground at similar range from the source. Podglajen et al. (2022) observed a similar improvements to detection when comparing ground- and balloon-based measurements from the 2022 Hunga Tonga eruption. It is also important to note that balloon-borne sensors float with the stratospheric winds and are not plagued by wind noise like ground-based stations. This, along with their placement within the AtmoSOFAR channel, gives them a marked advantage for detecting airborne sources.

4. Conclusions

Like the SOFAR channel in the ocean, it is theorized that an equivalent sound channel, the AtmoSOFAR, exists in the atmosphere. Such a channel would allow for meteoroid airbursts and supersonic vehicles passing through this region to be reliably sensed at vast distances using balloon-borne infrasound sensors. To test this hypothesis, we carried out a field test with the aim to record a ground truth airborne source (rocket) on an airborne infrasound sensor within the AtmoSOFAR channel. Infrasound signals from the ascent and descent of the rocket were recorded by the balloon-borne receiver. The successful detection of the infrasonic signals that traveled through the AtmoSOFAR channel marks the first such detection of a ground truth high-altitude source on an airborne infrasound sensor, and directly validates the presence of this duct. Compared to the ascent signal, the rocket's descent signal is larger and broadband due to the dynamics of the booster's return to Earth. We also noted a lack of detections at ground-based infrasound stations, both single sensor stations and arrays, located 313–1,303 km away. These results highlight the advantages of using balloon-borne infrasound sensors to detect these source types—a single airborne station can provide a detection while a single ground-based station may not.

10.1029/2023EA003149

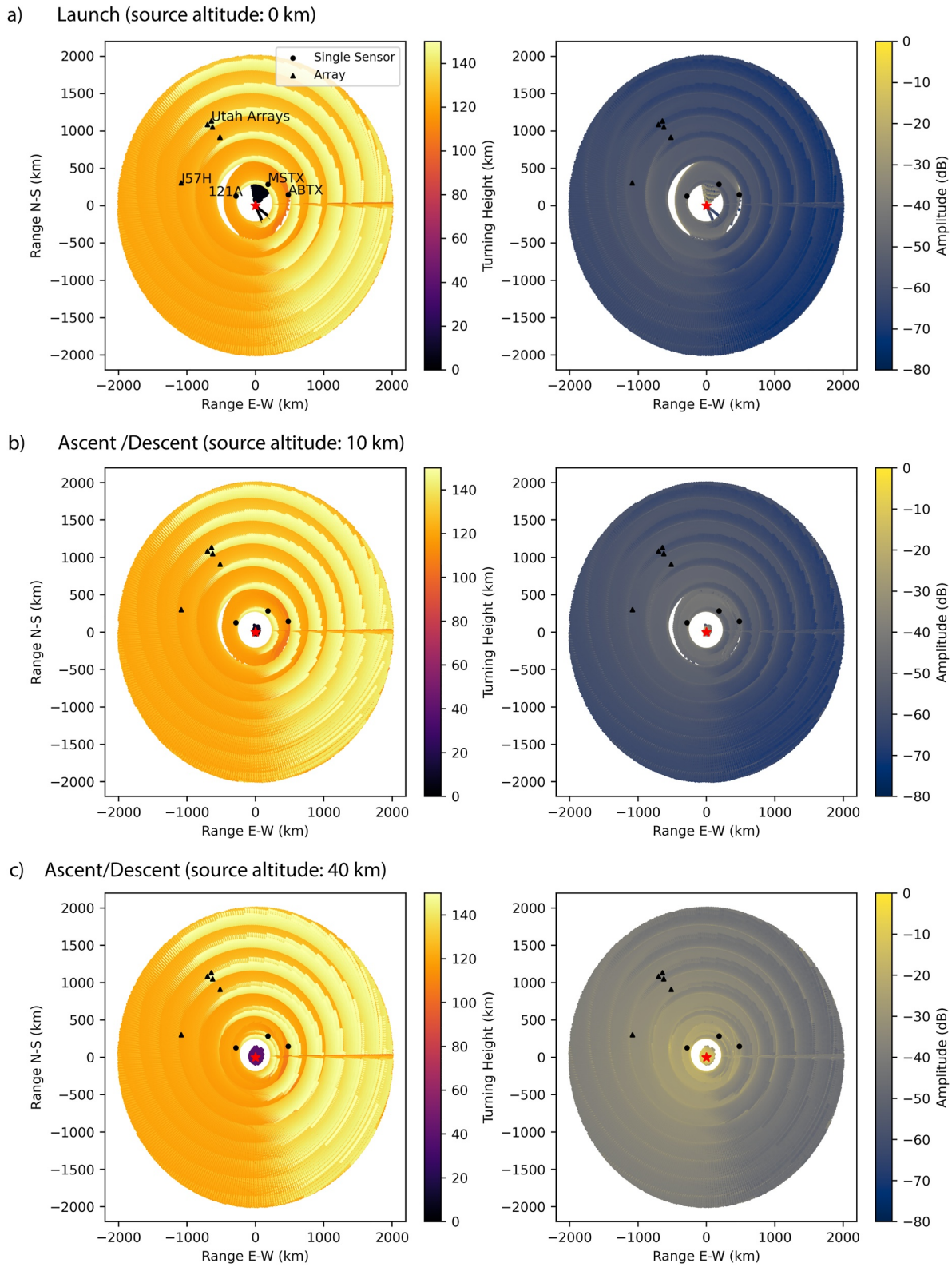

Figure 6. Propagation modeling for ground-based stations. All stations have turning heights in the thermosphere and are therefore unlikely to be detected. Amplitude loss is depicted on the right and supports the idea that signals will be too attenuated to be detected on ground stations.

10.1029/2023EA003149

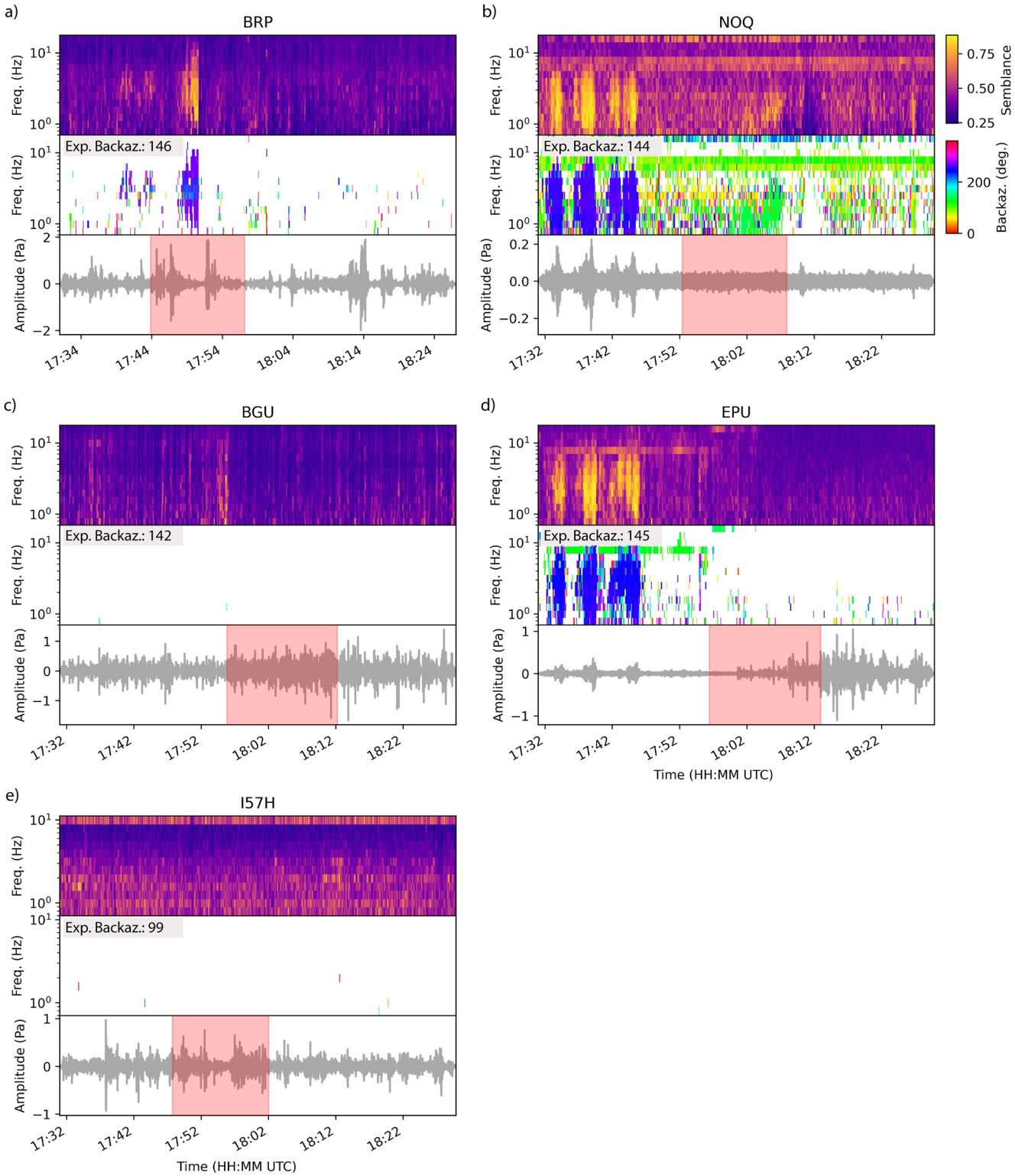

Figure 7. FK analysis for ground-based arrays. Blue Origin NS-15 arrivals may have been detected at NOQ, but are not present on any of the other stations.

Conflict of Interest

The authors declare no conflicts of interest relevant to this study.

Data Availability Statement

Ground-based infrasound data described in this work are freely available through the EarthScope Consortium Web Services at https://service.iris.edu/. Networks used included: University of Utah Regional Seismic Network (UU, University of Utah, 1962), New Mexico Tech Seismic Network (SC, New Mexico Tech, 1999), Central and Eastern US Network (N4, Albuquerque Seismological Laboratory/USGS, 2013), and International Miscellaneous Stations (IM, Various Institutions, 1965). Balloon trajectory and airborne infrasound data can be found at https://doi.org/10.5281/zenodo.8305719 (Albert et al., 2023). Figures were made with Matplotlib version 3.3.4 (Caswell et al., 2020; Hunter, 2007), available under the Matplotlib license at https://matplotlib.org/. InfraGA, the software used for infrasound propagation modeling in this study, is licensed under Los Alamos National Security, LLC (Blom, 2014) and is available on GitHub at https://github.com/LANL-Seismoacoustics/infraGA. Atmospheric profiles (Drob et al., 2003) are available through the National Center for Physical Acoustics and are available at http://g2s.ncpa.olemiss.edu/.

Acknowledgments

First, we extend our gratitude to Dr. Quentin Brissaud and an anonymous peer reviewer for their thoughtful comments and efforts towards improving this manuscript. The authors sincerely thank those who helped with preparing for and executing the solar balloon launches that made this research possible, specifically Benjamin Bishop, Erika Roesler, Michael Fleigle, Kathleen Hodgkinson, and Lauren Wheeler. This work was sponsored by the United States Department of Defense, Defense Threat Reduction Agency (DTRA) under the Nuclear Arms Control Technology (NACT) program. This article has been authored by an employee of National Technology & Engineering Solutions of Sandia, LLC under Contract DE-NA0003525 with the U.S. Department of Energy (DOE). The employee owns all right, title and interest in and to the article and is solely responsible for its contents. The United States Government retains and the publisher, by accepting the article for publication, acknowledges that the United States Government retains a non-exclusive, paid-up, irrevocable, world-wide license to publish or reproduce the published form of this article or allow others to do so, for United States Government purposes. The DOE will provide public access to these results of federally sponsored research in accordance with the DOE Public Access Plan https://www.energy.gov/downloads/doe-public-access-plan. This paper describes objective technical results and analysis. Any subjective views or opinions that might be expressed in the paper do not necessarily represent the views of the U.S. Department of Energy or the United States Government.

References

Alaska Volcano Observatory. (2016). Infrasound monitoring of volcanic eruptions in Alaska. Retrieved from https://www.avo.alaska.edu/about/infrasound.php

Albert, S., Bowman, D., Silber, E., & Dannemann Dugick, F. (2023). Airborne infrasound data from the AtmoSOFAR channel: First direct observations of an elevated acoustic duct (1.0) [Dataset]. Zenodo. https://doi.org/10.5281/zenodo.8305719

Albuquerque Seismological Laboratory/USGS. (2013). Central and eastern US network [Dataset]. International Federation of Digital Seismograph Networks. https://doi.org/10.7914/SN/N4

Anderson, J. F., Johnson, J. B., Bowman, D. C., & Ronan, T. J. (2018). The Gem infrasound logger and custom-built instrumentation. *Seismological Research Letters*, *89*(1), 153–164. https://doi.org/10.1785/0220170067

Arrowsmith, S. J., Tarin, S., & Albert, S. (2018). *Bloodhound 0.8: A Python package for infrasound data analysis* (No. SAND2018-9700). Sandia National Laboratories.

Blom, P. (2014). GeoAc: Numerical tools to model acoustic propagation in the geometric limit [Software]. Los Alamos National Laboratory. Retrieved from https://github.com/LANL-Seismoacoustics/infraGA

Blom, P., & Waxler, R. (2012). Impulse propagation in the nocturnal boundary layer: Analysis of the geometric component. *Journal of the Acoustical Society of America*, *131*(5), 3680–3690. https://doi.org/10.1121/1.3699174

Blue Origin. (2021). Replay - New shepard mission NS-15 webcast [video]. Retrieved from https://www.youtube.com/watch?v=domwsgorRW0

Bondár, I., Šindelářová, T., Ghica, D., Mitterbauer, U., Liashchuk, A., Baše, J., et al. (2022). Central and eastern European infrasound network: Contribution to infrasound monitoring. *Geophysical Journal International*, *230*(1), 565–579. https://doi.org/10.1093/gji/ggac06

Bowman, D. C. (2016). *Infrasound from ground to space*. The University of North Carolina at Chapel Hill.

Bowman, D. C., & Albert, S. A. (2018). Acoustic event location and background noise characterization on a free flying infrasound sensor network in the stratosphere. *Geophysical Journal International*, *213*(3), 1524–1535. https://doi.org/10.1093/gji/ggy069

Bowman, D. C., & Lees, J. M. (2016). Direct measurement of the acoustic wave field in the stratosphere. In *Proceedings of the 2016 IEEE aerospace conference*.

Bowman, D. C., & Lees, J. M. (2018). Upper atmosphere heating from ocean-generated acoustic wave energy. *Geophysical Research Letters*, *45*(10), 5144–5150. https://doi.org/10.1029/2018GL077737

Bowman, D. C., Lees, J. M., Cutts, J., Komjathy, A., Young, E., Seiffert, K., et al. (2018). Geoacoustic observations on drifting balloon-borne sensors. In *Infrasound monitoring for atmospheric studies* (pp. 475–507). Springer.

Bowman, D. C., Norman, P. E., Pauken, M. T., Albert, S. A., Dexheimer, D., Yang, X., et al. (2020). Multihour stratospheric flights with the Heliotrope solar hot-air balloon. *Journal of Atmospheric and Oceanic Technology*, *37*(6), 1051–1066. https://doi.org/10.1175/jtech-d-19-0175.1

Burlacu, V., Arrowsmith, S., Pankow, K. L., Hale, M. J., Hayward, C., & Stump, B. W. (2010). A network of infrasonic arrays in Utah. In *AGU fall meeting abstracts* (p. S11A-1922).

Caswell, T., Droettboom, M., Lee, A., Hunter, J., Firing, E., Stansby, D., et al. (2020). Matplotlib v3.3.4 [Software]. Zenodo. https://zenodo.org/record/4475376

Christie, D. R., & Campus, P. (2010). The IMS infrasound network: Design and establishment of infrasound stations. In *Infrasound monitoring for atmospheric studies* (pp. 29–77). Springer.

Drob, D. P., Picone, J. M., & Garces, M. (2003). Global morphology of infrasound propagation. *Journal of Geophysical Research*, *108*(D21), 4680. https://doi.org/10.1029/2002jd003307

Holton, J. R., Haynes, P. H., McIntyre, M. E., Douglass, A. R., Rood, R. B., & Pfister, L. (1995). Stratosphere-troposphere exchange. *Reviews of Geophysics*, *33*(4), 403–439. https://doi.org/10.1029/95rg02097

Hunter, J. D. (2007). Matplotlib: A 2d graphics environment. *Computing in Science & Engineering*, *9*(3), 90–95. https://doi.org/10.1109/MCSE.2007.55

Lawrence, M. W. (1999). Overview of the hydroacoustic monitoring system for the comprehensive nuclear-test ban treaty. *Journal of the Acoustical Society of America*, *105*(2_Supplement), 1037. https://doi.org/10.1121/1.424948

Marty, J. (2019). The IMS infrasound network: Current status and technological developments. In *Infrasound monitoring for atmospheric studies* (pp. 3–62). Springer.

New Mexico Tech. (1999). New Mexico Tech seismic network [Dataset]. International Federation of Digital Seismograph Networks. Retrieved from https://www.fdsn.org/networks/detail/SC/

Pilger, C., Ceranna, L., Le Pichon, A., & Brown, P. (2018). Large meteoroids as global infrasound reference events. In *Infrasound monitoring for atmospheric studies: Challenges in middle atmosphere dynamics and societal benefits* (pp. 451–470).

Podglajen, A., Le Pichon, A., Garcia, R. F., Gérier, S., Millet, C., Bedka, K., et al. (2022). Stratospheric balloon observations of Infrasound waves from the 15 January 2022 Hunga eruption, Tonga. *Geophysical Research Letters*, *49*(19), e2022GL100833. https://doi.org/10.1029/2022gl100833

Raspet, R., Abbott, J. P., Webster, J., Yu, J., Talmadge, C., Alberts, K., II, et al. (2019). New systems for wind noise reduction for infrasonic measurements. In *Infrasound monitoring for atmospheric studies* (pp. 91–124). Springer.

Rost, S., & Thomas, C. (2002). Array seismology: Methods and applications. *Reviews of Geophysics*, *40*(3), 2-1–2-27. https://doi.org/10.1029/2000rg000100

Silber, E. A., Bowman, D. C., & Ronac Giannone, M. (2023). Detection of the large surface explosion coupling experiment by a sparse network of balloon-borne infrasound sensors. *Remote Sensing*, *15*(2), 542. https://doi.org/10.3390/rs15020542

Silber, E. A., & Brown, P. (2019). Infrasound monitoring as a tool to characterize impacting near-earth objects (NEOs). In *Infrasound monitoring for atmospheric studies: Challenges in middle atmosphere dynamics and societal benefits* (pp. 939–986).

Silber, E. A., Le Pichon, A., & Brown, P. G. (2011). Infrasonic detection of a near-Earth object impact over Indonesia on 8 October 2009. *Geophysical Research Letters*, *38*(12). https://doi.org/10.1029/2011gl047633

Slad, G., & Merchant, B. J. (2021). *Evaluation of low cost infrasound sensor packages* (No. SAND2021-13632). Sandia National Lab. (SNL-NM).

Sutherland, L. C., & Bass, H. E. (2004). Atmospheric absorption in the atmosphere up to 160 km. *Journal of the Acoustical Society of America*, *115*(3), 1012–1032. https://doi.org/10.1121/1.1631937

University of Utah. (1962). University of Utah regional seismic network [Dataset]. International Federation of Digital Seismograph Networks. https://doi.org/10.7914/SN/UU

Various Institutions. (1965). International miscellaneous stations [Dataset]. International Federation of Digital Seismograph Networks. https://doi.org/10.7914/vefq-vh75

Weaver, R. L., & McAndrew, J. (1995). *The roswell report: Fact versus fiction in the New Mexico Desert*. U.S. Government Printing Office.

Wescott, J. W. (1964). *Acoustic detections of high-altitude turbulence*. The University of Michigan.

Young, E. F., Ballard, C., Garner, K., Von Hendy, M., Brown, P., Dougherty, E., et al. (2016). Detection of infrasound disturbances from the Earth's stratosphere. In *2016 IEEE aerospace conference* (pp. 1–9).

Young, E. F., Bowman, D. C., Lees, J. M., Klein, V., Arrowsmith, S. J., & Ballard, C. (2018). Explosion-generated infrasound recorded on ground and airborne microbarometers at regional distances. *Seismological Research Letters*, *89*(4), 1497–1506. https://doi.org/10.1785/0220180038